Commutation Torque Ripple Minimization in Direct Torque Controlled PM Brushless DC Drives

Y. Liu, Z.Q. Zhu, D. Howe
Department of Electronic and Electrical Engineering,
University of Sheffield, Mappin Street,
Sheffield S1 3JD, UK

Abstract — **This paper describes an improved implementation of direct torque control (DTC) to a permanent magnet brushless DC drive (BLDC). The commutation torque ripple, which occurs every 60° elec. in a conventional 3-phase BLDC machine, with 120° elec. 2-phase conduction, is reduced by employing a hybrid 2-phase and 3-phase switching mode during the commutation periods. It is based on the criterion of minimizing the torque error between the commanded torque and the estimated torque, and does not require knowledge of the conduction duration of the 3-phase switching mode. It adaptively adjusts the phase current waveform to maintain constant electromagnetic torque, so that commutation torque ripple, which would have resulted with existing DTC at high speeds, is effectively eliminated, as confirmed by both simulations and measurements.**

Keywords-Direct torque control, Permanent magnet motor, Current commutation, Torque ripple, BLDC drives

I. INTRODUCTION

Clearly, it is desirable to minimize torque ripple, since it may result in unacceptable speed ripple, vibration and acoustic noise. Ideally, a BLDC motor, with a trapezoidal back-emf waveform whose amplitude is constant over >120°elec. will produce ripple-free torque when supplied with rectangular 120°elec. phase currents. However, in a practical BLDC drive significant torque pulsations may arise due to the back-emf waveform departing from the ideal, phase current ripple resulting from commutation events and PWM, and cogging. Torque ripple due to phase current commutation is usually considered to be one of the main drawbacks of BLDC drives, compared to a brushless AC drives with sinusoidal back-emf and current waveforms. Hence, various researchers have investigated commutation torque ripple and proposed methods for its minimization [1-7]. In [1], it was shown that the commutation torque ripple might reach 50% of the average torque, but that it could be eliminated at low speed by employing current control based on direct current sensing. In [1][2], it was concluded that it could not be compensated for by current chopping in the 2-phase switching mode if the magnitude of the phase back-emf is >25% of the DC-link voltage. In [3], two methods for minimizing commutation torque ripple, viz. overlapping conduction, when all 3-phases carry current simultaneously for a short-period, and PWM chopping, were proposed. Although the first method was very simple, a torque ripple still resulted due to the difficulty of optimizing the overlapping time, which depends on the machine parameters and load and speed. The second method was essentially a current shaping PWM modulation, which significantly increased the system complexity and switching loss. An alternative explanation for the cause of commutation torque ripple was presented in [4], in which it was shown to result from the voltage between the neutral point of the inverter and the neutral point of the motor, which affects the phase current during commutation. The practical limitation of the bandwidth of the current controller was also considered. Hence, to achieve smooth torque, disturbing voltage compensation was adopted and a predictive term was added to compensate for the limited bandwidth. Adaptive torque ripple control for BLDC motors was proposed in [5], in which the phase current waveforms were shaped by the inner current control loop during commutation periods, while the outer speed control loop determined their magnitude. Both control loops enabled the torque ripple due to phase current ripple to be eliminated. A commutation torque ripple reduction method for low-cost applications was reported in [6]. The commutation interval was measured by monitoring the terminal voltage waveform without using a current sensor and the voltage disturbance rejection method was employed. Fourier series coefficients with space vector PWM were applied to the current control algorithm for minimizing torque ripple due to phase current commutation in a BLDC motor in [7].

However, in all the foregoing studies, torque ripple reduction was considered from the current control perspective so as to produce the required current reference, which was relatively complicated and not applicable to direct torque controlled BLDC drives. The application of DTC to a 3-phase BLDC drive operating in 120° elec. conduction mode was proposed in [8]. The authors extended the concept of DTC of a BLAC drive to a BLDC drive, which resulted in a simple control algorithm, reduced torque ripple, and direct flux control. They also compared the performance of a DTC controlled BLDC drive with that of a PWM current controlled drive, both with and without current shaping [9]. Since the torque, rather than the current, was controlled, the DTC controlled drive exhibited significantly less low-frequency torque ripple than the PWM current controlled drive without current shaping. It was also easier to implement and resulted in better torque control than the PWM current controlled drive with current shaping. Further, the influence of PWM and cogging on the steady-state performance of a direct torque controlled BLDC drive was investigated in [10]. It was shown

that the torque ripple and vibration of the motor were reduced significantly when unipolar PWM, rather than bipolar PWM, was employed, and the influence of the cogging torque was accounted for in the torque controller. However, the issue of commutation torque ripple was not addressed.

In this paper, an improved approach for reducing commutation torque ripple in direct torque controlled BLDC drives is proposed. The commutation torque ripple is analyzed, based on the approach which was presented in [1], and is minimized by combining the conventional 2-phase switching mode with a controllable 3-phase switching mode during periods when the current is being commutated. It differs from the current control method in [3] in that the exact duration of the 3-phase switching mode is not required since it is automatically determined by comparing the commanded torque with the estimated torque in DTC. Its effectiveness is validated by both simulations and measurements.

II. Analysis of Commutation Torque Ripple in DTC BLDC Drive

Idealised back-emf and current waveforms for a 120° elec. conduction mode, 3-phase BLDC drive are shown in Fig. 1. Since it can produce a higher electromagnetic torque per ampere than that which results with 3-phase, 180° elec. conduction, it is the most commonly used mode, and, hence, is considered in this paper. The principle of DTC when applied to a BLDC drive is described in [8]. In this section, the current and torque ripple which result due to commutation events in a 120° elec. conduction, 3-phase, star-connected, BLDC drive are analyzed, in a similar way to that given in [1]. A controllable 3-phase switching mode is then introduced during the commutation periods and the resulting current and torque ripple are analyzed. Finally, the two operating modes are combined to minimize the commutation torque ripple in a direct torque controlled BLDC drive.

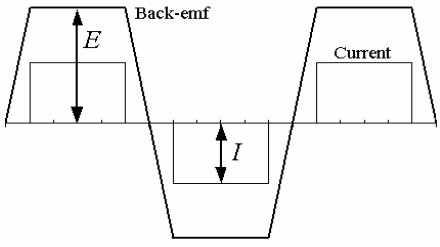

Fig. 1 Idealised back-emf and current waveforms in BLDC drive.

The stator phase voltage equations can be simplified as:

$$u_{an} = i_a R_s + e_a + L_s \frac{di_a}{dt} \tag{1}$$

$$u_{bn} = i_b R_s + e_b + L_s \frac{di_b}{dt} \tag{2}$$

$$u_{cn} = i_c R_s + e_c + L_s \frac{di_c}{dt} \tag{3}$$

where u_{an}, u_{bn}, u_{cn}, e_a, e_b, e_c, i_a, i_b, i_c are the phase voltages, back-emfs and currents of phases a, b, c, respectively, and R_s and L_s are the stator winding resistance and inductance, respectively. However, the winding resistance is neglected to simplify the analysis. The equations for the phase winding terminal to ground (n_0) voltages, u_{an0}, u_{bn0}, u_{cn0}, are:

$$u_{an0} = u_{an} + u_{nn0} \tag{4}$$

$$u_{bn0} = u_{bn} + u_{nn0} \tag{5}$$

$$u_{cn0} = u_{cn} + u_{nn0} \tag{6}$$

where u_{nn0} is the neutral point to ground voltage.

The sum of the phase winding terminal to ground voltages is:

$$\begin{aligned} u_{an0} + u_{bn0} + u_{cn0} &= u_{an} + u_{bn} + u_{cn} + 3u_{nn0} \\ &= e_a + e_b + e_c + 3u_{nn0} \end{aligned} \tag{7}$$

Thus, the neutral point to ground voltage is:

$$u_{nn0} = \frac{1}{3}(u_{an0} + u_{bn0} + u_{cn0} - e_a - e_b - e_b) \tag{8}$$

Based on the above equations, the phase current commutation process can be analyzed. Fig. 2 shows the current paths during commutation between phases b and c when the switching states change from (100100) to (100001), where the digits are logical values which describe the states ("1" indicates on and "0" indicates off) of the upper and lower switches for phases a, b, and c, respectively. At the instant of phase current commutation, the three phase back-emfs are e_a=E, e_b=-E and e_c=-E, where E is the peak value of the back-emf waveform, Fig.1. The back-emfs are assumed to be constant during phase current commutation as in [1], although this is clearly not the case, as is evident from Fig.1. During commutation, Fig. 2(b), the rate of change of the phase currents is determined from the voltage equations:

$$\frac{di_a}{dt} = \frac{1}{3L_s}U_{dc} - \frac{4}{3L_s}E \tag{9}$$

$$\frac{di_b}{dt} = \frac{1}{3L_s}U_{dc} + \frac{2}{3L_s}E \tag{10}$$

$$\frac{di_c}{dt} = -\frac{2}{3L_s}U_{dc} + \frac{2}{3L_s}E \tag{11}$$

where U_{dc} is the DC-link voltage.

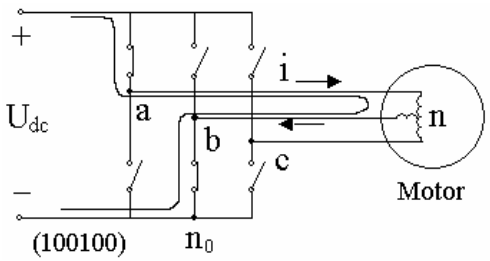

(a) Before current commutation

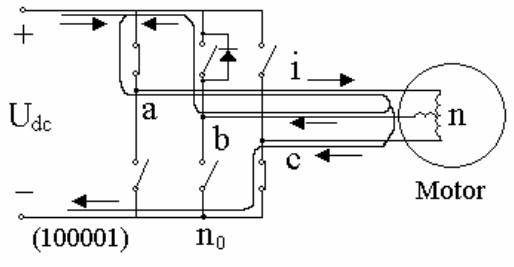

(b) During current commutation

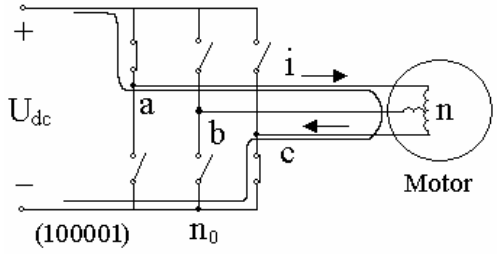

(c) After current commutation

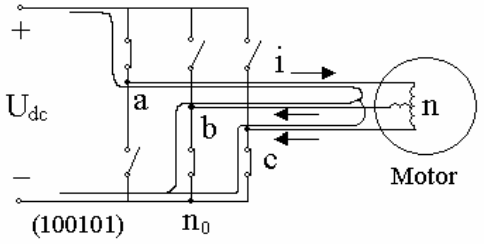

(d) Current commutation in 3-phase switching mode

Fig. 2 Switching states during current commutation.

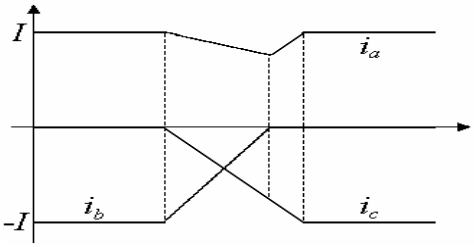

(a) $\left|\frac{di_b}{dt}\right| > \left|\frac{di_c}{dt}\right|$, i.e. $U_{dc}<4E$

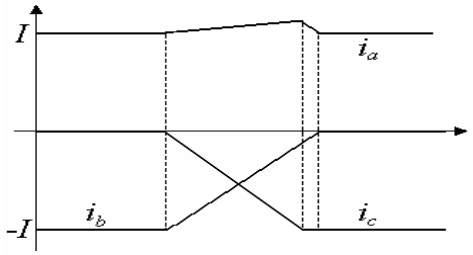

(b) $\left|\frac{di_b}{dt}\right| < \left|\frac{di_c}{dt}\right|$, i.e. $U_{dc}>4E$

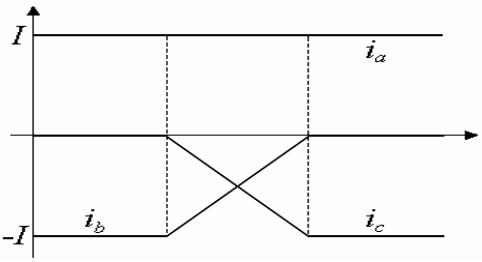

(c) $\left|\frac{di_b}{dt}\right| = \left|\frac{di_c}{dt}\right|$, i.e. $U_{dc}=4E$

Fig. 3 Current variation during current commutation.

As shown in Fig.3, three conditions determine the phase current variation during commutation [1].

(a) When $\left|\frac{di_b}{dt}\right| > \left|\frac{di_c}{dt}\right|$, Fig. 3(a), i.e. $\frac{di_b}{dt} > -\frac{di_c}{dt}$. Therefore,

$$\frac{1}{3L_s}U_{dc}+\frac{2}{3L_s}E > \frac{2}{3L_s}U_{dc}-\frac{2}{3L_s}E \tag{12}$$

Thus, $U_{dc} < 4E$, and $\frac{di_a}{dt} < 0$, i.e. the current in phase *a* decreases.

(b) When $\left|\frac{di_b}{dt}\right| < \left|\frac{di_c}{dt}\right|$, Fig.3 (b), i.e. $\frac{di_b}{dt} < -\frac{di_c}{dt}$. Therefore,

$$\frac{1}{3L_s}U_{dc}+\frac{2}{3L_s}E < \frac{2}{3L_s}U_{dc}-\frac{2}{3L_s}E \tag{13}$$

Thus, $U_{dc} > 4E$, and $\frac{di_a}{dt} > 0$, i.e. the current in phase *a* increases.

(c) When $\left|\frac{di_b}{dt}\right| = \left|\frac{di_c}{dt}\right|$, Fig.3 (c), i.e. $\frac{di_b}{dt} = -\frac{di_c}{dt}$. Therefore,

$$\frac{1}{3L_s}U_{dc}+\frac{2}{3L_s}E = \frac{2}{3L_s}U_{dc}-\frac{2}{3L_s}E \tag{14}$$

Thus, $U_{dc} = 4E$, and $\frac{di_a}{dt} = 0$, i.e. the current in phase *a* is constant.

When the motor is operating at low speed ($U_{dc}>4E$), the rate of rise of the current i_c in phase *c* during commutation can be reduced by current chopping so that it has the same rate of change as the current i_b in phase *b* and reaches its final steady-state value at the same instant that phase b is commutated off, while maintaining the current i_a in the non-commutated phase *a* constant.

However, when the motor is operating at high speed ($U_{dc}<4E$), the rate of decrease of the current i_b in phase *b* during commutation, which is associated with the conduction of the free-wheel diode, will be so high that the rate of increase

of phase *c* current i_c cannot be increased sufficiently even if the DC link voltage is fully utilized.

In order to maintain i_a constant during high speed operation, the instant at which phase *b* is commutated off can be delayed and the machine can be operated in 3-phase switching mode, as illustrated in Fig. 2 (d). The three phase currents will then be fully controllable throughout the commutation period, i.e. the uncontrollable commutation period, which is associated with the conduction of free-wheel diode, is now controllable. Hence, this concept is utilized to achieve improved DTC of the BLDC drive. The time which is taken for the current in phase *b* to decay to zero can be extended by controlling the switching of phase *b* via PWM, i.e. the usual 2-phase switching mode is combined with a controllable 3-phase switching mode during commutation periods. The period during which the 3-phase switching mode is employed is determined by the criterion of torque error, ΔT, between the commanded torque and the estimated torque so as to minimize the torque ripple during commutation. Thus, during commutation when $\Delta T \le \Delta T^*$, the 2-phase switching mode is employed, and when $\Delta T > \Delta T^*$, the 3-phase switching mode is employed, where ΔT^* is a pre-specified limit for the torque ripple. Thus, by employing this hybrid 2-phase and 3-phase switching mode, the electromagnetic torque is maintained constant and commutation torque ripple which would otherwise result from the uncontrollable conduction of the free-wheel diodes in conventional 2-phase switching mode during commutation is minimized. In addition, there is no need to calculate the duration of the 2-phase switching mode or the 3-phase switching mode since the change from one to other is automatic according to the torque error.

In a practical implementation, ΔT^* is set to zero for simplicity, and the actual torque ripple is determined by the system control frequency. Clearly, however, the shorter the control cycle the lower the torque ripple, although the switching frequency will be higher.

It is worth mentioning that during the 3-phase switching mode the switching states are exactly the same as those which would be applied in 3-phase, 180° elec. conduction BLDC operation, and as shown in Fig. 2 (d), i_a increases towards a positive value, while i_b and i_c increase towards negative values. Since in this case $U_{dc}>2E$ at any instant, the rate of change of the three phase currents can be expressed as:

$$\frac{di_a}{dt} = \frac{2}{3L_s}U_{dc} - \frac{4}{3L_s}E \qquad \text{(+ve value)} \qquad (15)$$

$$\frac{di_b}{dt} = -\frac{1}{3L_s}U_{dc} + \frac{2}{3L_s}E \qquad \text{(-ve value)} \qquad (16)$$

$$\frac{di_c}{dt} = -\frac{1}{3L_s}U_{dc} + \frac{2}{3L_s}E \qquad \text{(-ve value)} \qquad (17)$$

Therefore, it can be concluded that during the commutation period the current i_a in the non-commutated phase increases when $U_{dc}>4E$ and decreases when $U_{dc}<4E$. Similarly for the electromagnetic torque, since this is proportional to the product of the back-emf and the phase current. Nevertheless, when the machine runs at low speed ($U_{dc}>4E$), PWM can still maintain the current more or less constant in the non-commutated phase constant. More importantly, when the machine runs at high speed ($U_{dc}<4E$), the rate of change of the decreasing current is reduced by the 3-phase switching mode so that the influence of the two commutating currents is cancelled and they attain the final steady-state values at the same instant of time. Thus, during the commutation periods of a 120°elec. 2-phase conduction BLDC drive, the proposed DTC scheme will automatically employ the conventional 2-phase conduction (i.e. with uncontrolled commutation via the uncontrollable free-wheeling diode) at low speeds ($U_{dc}\ge 4E$), and the hybrid 2-phase and 3-phase switching modes at high speeds ($U_{dc}<4E$), so that commutation torque ripple is minimized throughout the entire operating speed range.

III. Simulated and Measured Results

Fig. 4 shows measured phase and line back-emf waveforms of a 3-phase, 10-pole, 12-slot, BLDC motor whose parameters are given in Table I. The improved DTC strategy has been implemented on a TMS320C31 DSP, and the simulation model which was used to predict the drive performance was implemented using Matlab/Simulink. The DC link voltage U_{dc} = 36V, and when $U_{dc} \approx 4E$, the motor speed is ~260rpm. The measured electromagnetic torque waveforms are obtained from the torque observer in the DTC system. The DSP control period is 50 μs.

Figs.5 and 6, and 7 and 8, show simulated and measured phase current and electromagnetic torque waveforms when the motor runs at low speed (200rpm) and high speed (400rpm), respectively, without compensating for commutation torque ripple. As will be seen, commutation torque ripple is negligible at low speed, but it is clearly apparent at high speed.

TABLE I. Parameters of Surface-Mounted PM Brushless Motor

Number of poles, p	10
DC link voltage (V)	36
Rated speed (rpm)	400
PM excitation flux-linkage (Wb)	0.0794
Phase resistance (Ω)	0.35
Self-inductance (mH)	3.9
Mutual-inductance (mH)	0.0023

Figs. 9 and 10 compare the simulated and measured performance which results with the improved DTC when the motor is running at high speed (400rpm). As will be seen, since the uncontrollable free-wheel diode conduction commutation period is made controllable in the improved DTC, the commutation torque ripple is reduced. The effect of PWM during the commutation period is clearly evident in the phase

winding terminal to ground voltage waveforms, Figs. 9(a) and 10 (a). In contrast, as shown in Figs. 6(a) and 8(a), there is no PWM during the commutation periods with uncontrollable free-wheel diode conduction. Since the 3-phase switching mode is automatically applied during commutation of the phase currents, its exact duration is not required and the phase current waveforms are adaptively optimized simply by comparing the commanded torque and the estimated torque. Hence, it is much easier to implement than the method presented in [3], which required accurate knowledge of the time for which the currents in the phases undergoing commutation should overlap. It can be seen that, at the instant of commutation, the improved DTC results in the current in the phase which is not undergoing commutation, Figs.9(a) and 10(a), being slightly higher than that which results with the existing DTC, Figs. 6(b) and 8(b). As a result, the commutation torque ripple is successfully eliminated, as confirmed by both the simulated and measured results shown in Figs. 9(c) and 10(c).

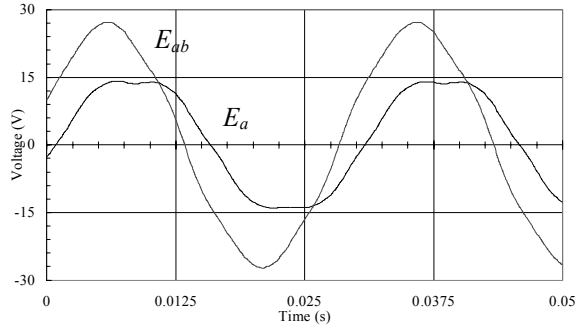

Fig. 4 Phase and line back-emf waveforms (400rpm).

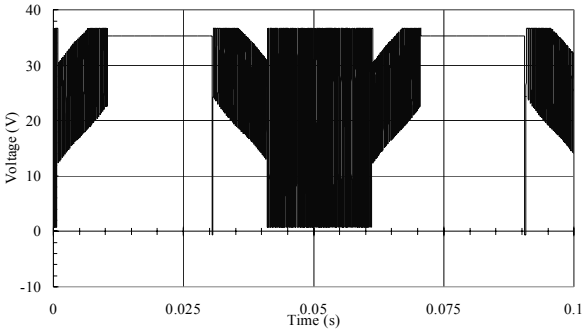

(a) Phase winding terminal to ground voltage

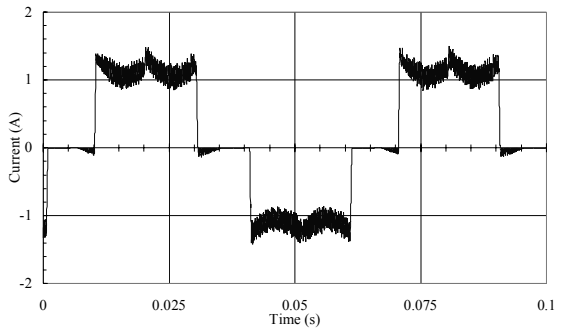

(b) Phase current

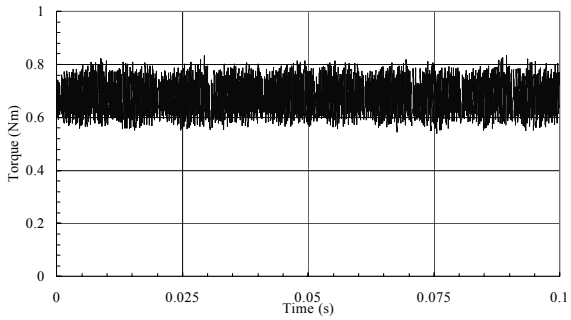

(c) Electromagnetic torque

Fig.5 Simulated performance with conventional DTC at low speed (200rpm).

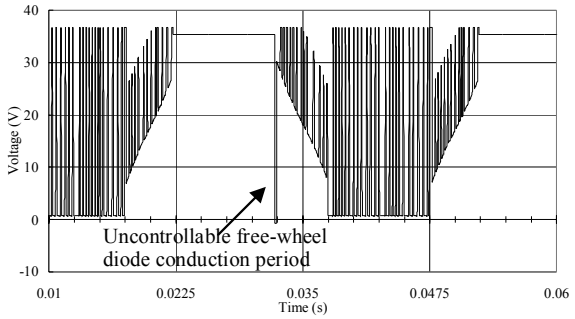

(a) Phase winding terminal to ground voltage

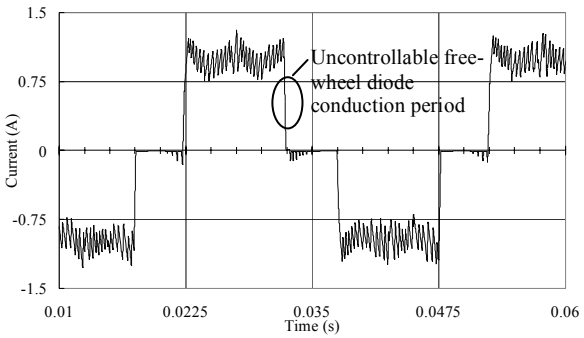

(b) Phase current

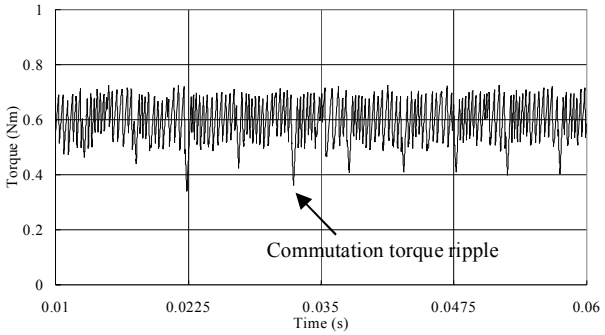

(c) Electromagnetic torque

Fig.6 Simulated performance with conventional DTC at high speed (400rpm).

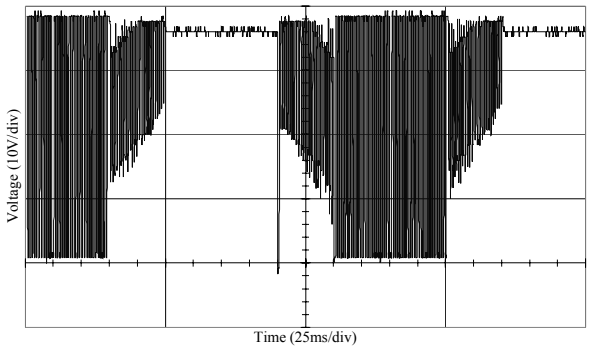

(a) Phase winding terminal to ground voltage

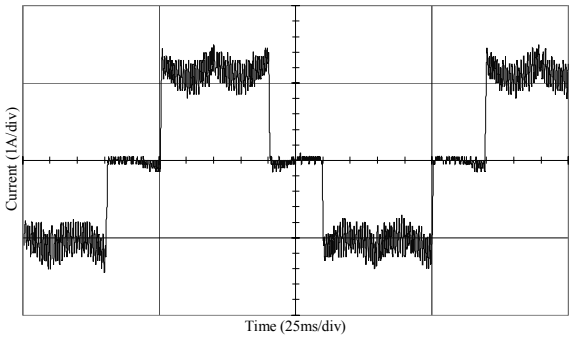

(b) Phase current

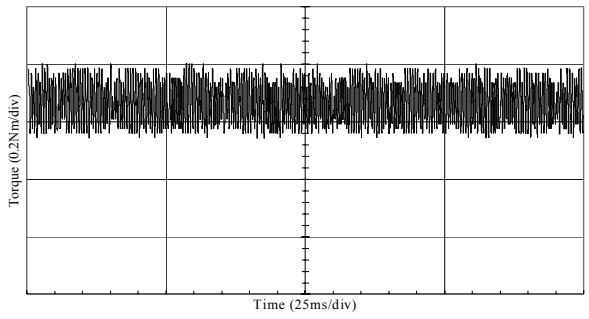

(c) Electromagnetic torque

Fig.7 Measured performance with conventional DTC at low speed (200rpm).

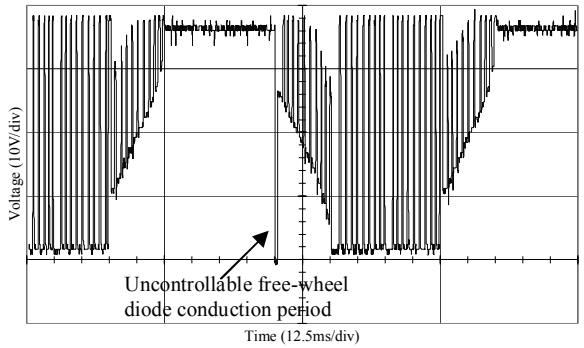

(a) Phase winding terminal to ground voltage

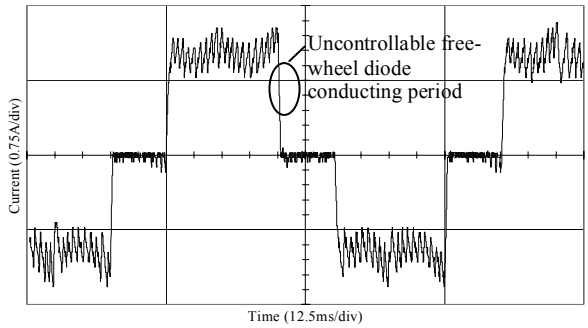

(b) Phase current

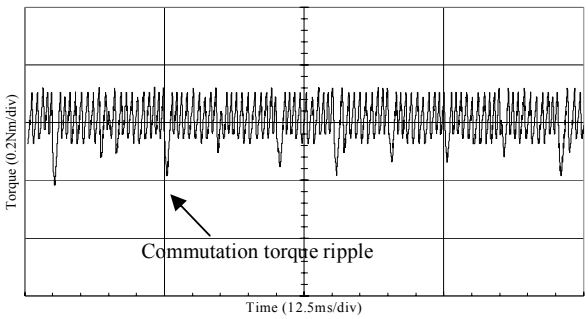

(c) Electromagnetic torque

Fig.8 Measured performance with conventional DTC at high speed (400rpm).

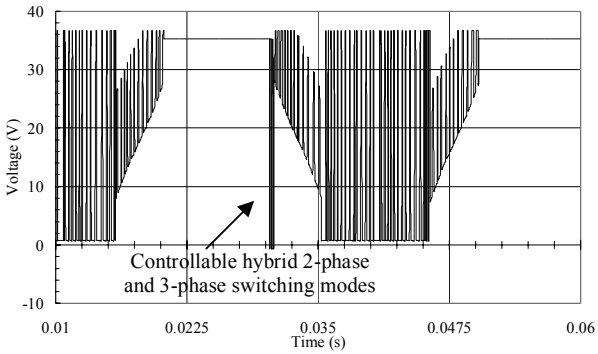

(a) Phase winding terminal to ground voltage

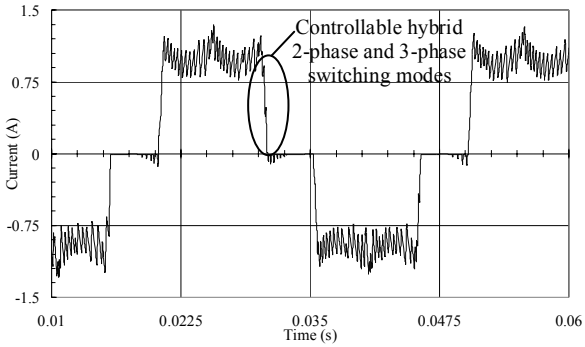

(a) Phase current

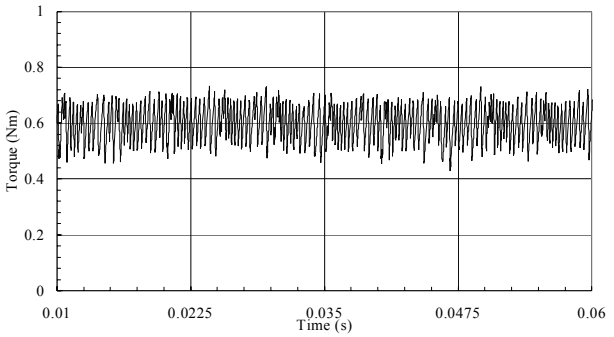

(b) Electromagnetic torque

Fig.9 Simulated performance with improved DTC at high speed (400rpm).

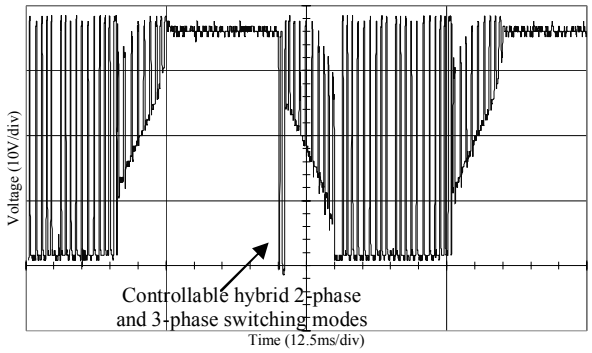

(a) Phase winding terminal to ground voltage

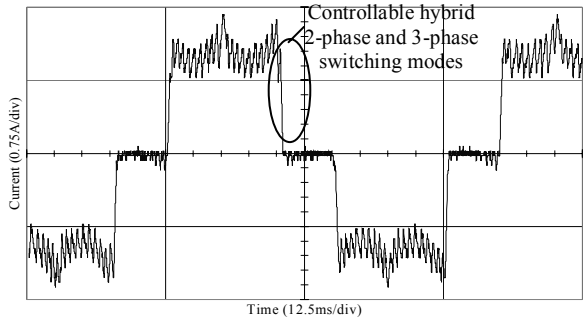

(b) Phase current

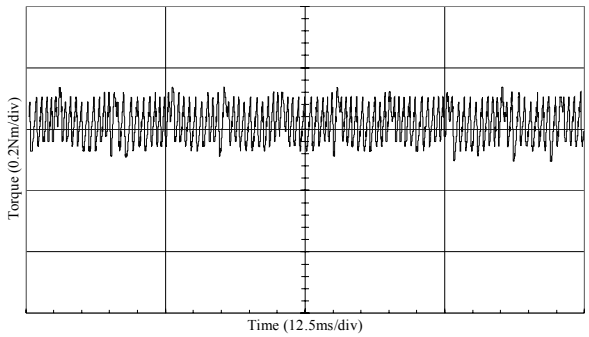

(c) Electromagnetic torque

Fig.10 Measured performance with improved DTC at high speed (400rpm).

IV. CONCLUSIONS

The phase current waveform and torque ripple which result during commutation events in a direct torque controlled 120° elec. 2-phase conduction permanent magnet brushless DC drive have been analyzed, and an improved DTC strategy has been proposed to minimise the commutation torque ripple. During commutation periods at high rotational speeds, it combines the 2-phase and 3-phase switching modes which are automatically implemented by minimizing the torque error between the commanded torque and the estimated torque, and the torque ripple due to commutation events is reduced significantly, as has been demonstrated by both simulations and measurements.

REFERENCES

[1] R. Carlson, M. Lajoie-Mazenc and J. C. D. S. Fagundes, "Analysis of torque ripple due to phase commutation in brushless DC machines," *IEEE Trans. on Industry Applications*, Vol.28, no.3, May-June 1992, pp.632-638.

[2] H. Tan, "Controllability analysis of torque ripple due to phase commutation in brushless DC motors," *Proc. of 5th Int. Conf. on Electrical Machines and Systems*, Vol.2, 18-20 Aug. 2001, pp.1317-1322.

[3] Y. Murai, Y. Kawase, K. Ohashi, K. Nagatake and K. Okuyama, "Torque ripple improvement for brushless DC miniature motors," *IEEE Trans. on Industry Applications*, vol.25, No.3, May-June 1989, pp.441-450.

[4] C. S. Berendsen, G. Champenois and A. Bolopion, "Commutation strategies for brushless DC motors: influence on instant torque," *IEEE Trans. on Power Electronics*, Vol. 8, No.2, April 1993, pp.231-236.

[5] Y. Sozer and D. A. Torrey, "Adaptive torque ripple control of permanent magnet brushless DC motors," *Proc. 13th Annual Applied Power Electronics Conference and Exposition*, Vol.1, 15-19 Feb. 1998, pp.86-92.

[6] D. K. Kim, K. W. Lee and B. I. Kwon, "Torque ripple reduction method in a sensorless drive for the BLDC motor," *Korean IEE Int. Trans. on Electrical Machinery and Energy Conversion Systems,* Vol.4-B, No.4, pp.196-200, 2004.

[7] T. S. Kim, S. C Ahn and D. S. Hyun, "A new current control algorithm for torque ripple reduction of BLDC motors," *Proc. of 27th Annual Conference of the IEEE Industrial Electronics Society*, Vol. 2, 29th Nov.-2nd Dec. 2001 pp.1521-1526.

[8] Y. Liu, Z. Q. Zhu and D. Howe, "Direct torque control of brushless DC drives with reduced torque ripple," *IEEE Trans. on Industry Applications*, Vol.41, No.2, March/April, 2005, pp.599-608.

[9] Z.Q. Zhu, Y. Liu, and D. Howe, "Comparison of performance of brushless DC drives under direct torque control and PWM current control," *Korean IEE Int. Trans. on Electrical Machinery and Energy Conversion Systems*, Vol.5-B, No.4, 2005, pp.337-342.

[10] Z.Q. Zhu, Y. Liu, and D. Howe, "Steady-state dynamic performance of a direct torque controlled PM brushless DC drive accounting for influence of PWM chopping and cogging torque," *IEE Int. Conf. on Power Electronics, Machines and Drives*, 4-6 April 2006, Dublin, Ireland, pp. 556-560.